

Phase locking to the n -torus

Peter Grindrod CBE and Ebrahim L. Patel

Mathematical Institute, University of Oxford, Oxford OX2 6GG, UK

March 28, 2016

Abstract

We discuss phase resetting behaviour when non-small, near instantaneous, perturbations are applied to a dynamical system containing a strong attractor that is equivalent to a winding map on an n -dimensional torus. Almost all of the literature to date has focused on the application of phase transition curves derivable for systems with attracting limit cycles, when $n = 1$, and the consequent possibilities for entrainment of the system subject to such periodic largish perturbations. In higher dimensions the familiar tongues in the amplitude versus period plane, describing solutions entrained with periodic fast perturbations, have subtle structure (since only locally two dimensional subsets of the n -dimensional torus may admit such solutions) while the topological class of the n -dimensional phase transition mapping is represented by a matrix of winding numbers. In turn this governs the existence of asymptotic solutions in the limits of small perturbations. This paper is an attempt to survey the entrainment behaviour for the full set of alternative (near rigid) phase transition mappings definable on the 2-torus. We also discuss higher dimensional effects and we suggest how this might be important for nonlinear neural circuits including delays that routinely exhibit such attractors and may drive one another in cascades of periodic behaviour. Phase transition mapping, n -tori attractors, periodic entrainment, delay differential equations.

1 Introduction: phase transitions for clocks and tori

We consider a class of dynamical systems containing a hyperbolic invariant torus such that local trajectories (within some attracting basin) are all subject to a very *fast* dynamic that pulls them towards the torus, relative to a *slow* dynamic of the trajectories on, and very close to, the torus which results in its periodic (phase) coordinates simply increasing in a monotonic manner. We wish to investigate what happens when trajectories within the

attracting torus are subject to near instantaneous (impulsive or *very fast*) state-space perturbations (from some external process). These perturbations may be large compared to the scale of the torus, but once completed we shall assume that the state remains within the basin of attraction, and that consequently the trajectory starting from that perturbed state returns rapidly back onto the torus. The result is that the toroidal phase is instantaneously transitioned from where it was prior to the state perturbation to where it arrives post both perturbation and rapid return. For example see Figure 1, where the attractor is subject to a rigid impulse transformation followed by a fast return in the standard toroidal radial coordinate (while preserving the toroidal phase coordinates).

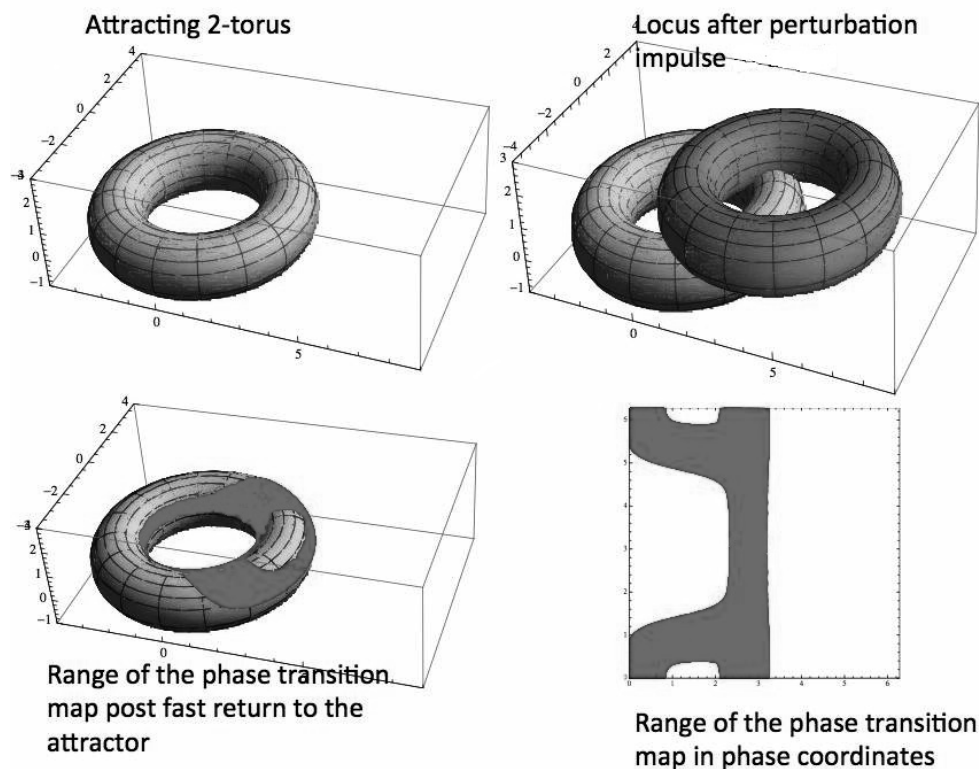


Figure 1: An invariant 2- torus (top left) in \mathbb{R}^3 ; its image after impulse perturbations applied to all points (top right), resulting in a rigid translation of 3.5 units in the x direction and 1.25 units in the z direction; the range of the transition map (shaded in bottom left) following the fast return to the attractor (in the radial toroidal coordinate) and shown on the two toroidal phase coordinates (bottom right). The result indicates there is no cycling of one of the image phase co-ordinates as either of the original phases are cycled. This phase transition map is clearly not homotopic to the identity.

We will not assume small system perturbations (for example, small de-

formations to integrable Hamiltonian systems). Instead our framework is a generalisation of the phase transition behaviour observed for *clocks* (which are represented by stable limit cycles) that are subject to impulses. In such situations we consider the perturbation happening at any and all points on the limit cycle, resulting in a range locus, and then map that locus back onto the original limit cycle, relying on a fast radial component of the flow.

The canonical clock example, introduced by Glass and Mackey (1988), assumes the unit circle as the attractor, and the circle map, $M : S^1 \rightarrow S^1$, where ϕ is a 2π periodic coordinate and

$$\cos M(\phi) = \frac{b + \cos \phi}{\sqrt{1 + b^2 + 2b \cos \phi}} \quad \text{and} \quad \sin M(\phi) = \frac{\sin \phi}{\sqrt{1 + b^2 + 2b \cos \phi}}.$$

This particular map is the result of a perturbation of size b in the $\phi = 0$ direction, off the unit circle, followed by a phase preserving return to the closest point on the unit circle. The perturbed image is thus a unit circle shifted by an amount b in the $\phi = 0$ direction; while the fast radial return is well-defined providing the perturbed image locus does not include the origin which is an unstable rest point (that is $b \neq 1$). For $0 \leq b < 1$ M is invertible and is called a Type-1 map since the post-transition phase, $\phi' = M(\phi)$, winds through exactly one cycle as the pre-transition phase, ϕ , moves through a single cycle itself (this terminology was introduced by Winfree (2001)). In that case M may be written as $M(\phi) = \phi + F(\phi)$ where F is continuous and 2π -periodic. If $b > 1$ then M becomes a Type-0, non-invertible, phase resetting mapping, since $\phi' = M(\phi)$ winds through exactly zero cycles as ϕ moves through a single cycle. In that case M itself is continuous and 2π -periodic, and its range lies within $[-\pi/2, \pi/2]$.

Now, continuing with this example, suppose that without any perturbations there is a simple dynamic on S^1 given by $\dot{\phi} = 1$, which simply winds uniformly around the circle. We wish to consider the situation where an instantaneous perturbation given by M is applied periodically and use our knowledge of the corresponding phase resetting behaviour so as to decide if there is a solution which is phase locked to the period of the applied perturbations.

When the perturbation is applied periodically, every p units of time, we have a p -periodic solution at ϕ if and only if $\cos(p + M(\phi)) = \cos \phi$.

For $b = 0$ it follows that $p = 2\pi k$ for any integer k , and ϕ is unrestricted (all values lead to a phase-locked p -periodic solution). Fixing ϕ , we may expand p out as a regular series in $b > 0$. We obtain $p - 2\pi k = b \sin \phi - \frac{b^2}{2} \sin 2\phi + \frac{b^3}{3} \sin 3\phi - \frac{b^4}{4} \sin 4\phi + \dots$. As we vary $\phi \in [0, 2\pi)$ these curves together parametrize the familiar Arnold tongue, shown in Figure 2 with curved lines showing constant values for ϕ . Since it appears to be previously unpublished we note in passing that this series solution results in

the following closed form:

$$p - 2\pi k = \frac{1}{2} \left(-\tan^{-1} \left(\frac{(1-b)\tan\frac{\phi}{2}}{b+1} \right) - \tan^{-1} \left(\frac{\sin\phi}{b+\cos\phi} \right) + \frac{3\phi}{2} \right).$$

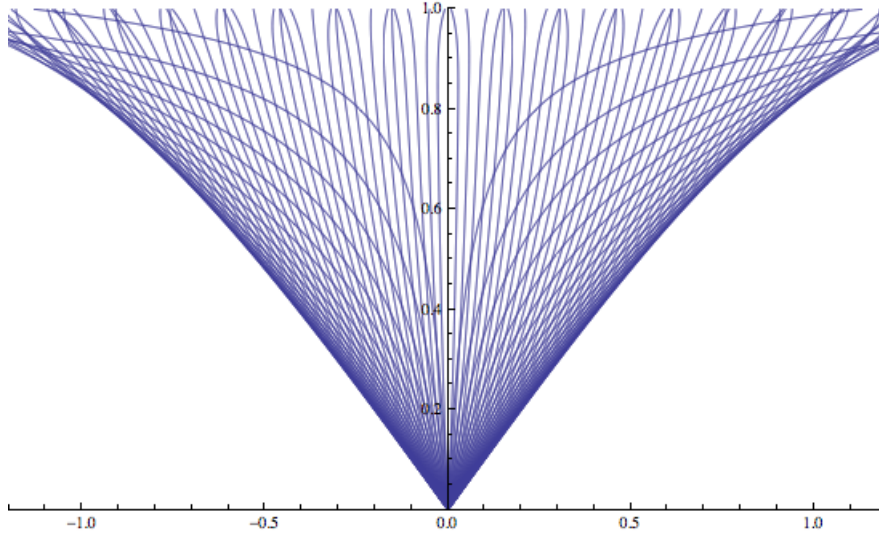


Figure 2: b versus $p - 2\pi k$ for a range of ϕ values.

On the other hand when a Type-0 perturbation ($b > 1$) is applied p -periodically we can have a periodic solution for all p , satisfying $\phi = p + M(\phi)$. Here M is 2π -periodic, continuous and bounded, so there always exists at least one solution (modulo 2π).

Notice that if we only consider b -small perturbations, which are Type 1, we never observe anything like the b -large type behaviour, and vice versa. Hence, for clocks at least, the homotopy type of the phase transition map dominates the nature of possible phase entrainment; see MacKay (1991).

The literature on phase resetting for dynamical systems that possess attracting limit cycles (clocks) is abundant with examples from the highly abstracted phase system models (caricatures) to more detailed and realistic physiochemical models for neural oscillators and other applications beyond. When collections of such systems are to be coupled together or, more prosaically, where an oscillatory signal in the form of a phase resetting impulse-stimulus drives such an oscillatory system, the entrainment between the forcing term and system's response is embodied by the phase response curve (PRC, the advancement or retardation of the attractor's phase as a function of its phase immediately prior to a single impulse perturbation) or equivalently the phase transition curve (PTC, the attractors' phase immediately post perturbation as a function of its phase immediately prior to a single impulse perturbation). The body of research and its applications, most notably

to coupled neural systems, has greatly contributed to the understanding of emergent behaviour of coupled oscillatory systems, nowadays often called complex systems.

The questions addressed for individual systems are usually of four types: (i) the characterization of their oscillatory behaviour and, in particular, the alternative modes of birth of limit cycles; (ii) the investigation of their corresponding PTCs; (iii) the investigation of their response when periodically forced by ‘upstream’ stimuli, and hence of the system’s ability to become entrained, with such periodic forcing; and (iv) the investigation of such behaviour for aggregates and networks of multiple similar instances of such systems subject to pairwise (directed) coupling. See Brown et al. (2004); Ermentrout (1996); Ermentrout and Kopell (1990); Glass and Mackey (1988); Goel and Ermentrout (2002); Guevara et al. (1986); Rinzel and Ermentrout (1989) and the references therein.

In this paper we have nothing to add to the body of knowledge concerning forced and coupled oscillatory systems containing an attracting hyperbolic periodic orbit with local isochrons. Instead we shall consider the situation where the underlying dynamical system has an attracting set that is an invariant torus of dimension $n > 1$, and consequently has n -phase variables, with n -dimensional phase, ϕ , satisfying $\dot{\phi} = \omega$, some strictly positive constant vector. We wish to examine how possibly large state-space perturbations (but not so large as to leave the basin of attraction) result in a set of 2^{n^2} homotopy types of phase transition map (even while assuming the perturbation map itself is relatively rigid), and thus there is a range of possible phase entrainment behaviours, when the perturbations are applied periodically in time. We limit ourselves to a classification of the maps according to existence of fixed points because, as we show, this provides sufficiently rich dynamics; the general case is therefore beyond the scope of our aims.

Returning to the general n -dimensional setting, for small perturbations of tori we may dispense with the assumption of *fast* perturbations and *fast* returns, since the phase transition map will be close to the identity mapping. Yet for large enough perturbations the image of the transition map will be restricted to some subset of the torus and thus the phase transition mapping’s homotopy type is less trivial. So we expect that the ability of the system to resonate (to entrain) with periodically applied perturbations will depend on the homotopy type of the transition mapping.

Since we consider hyperbolic attracting tori a Hamiltonian context is not relevant to this paper. However Kolmogorov-Arnold-Moser theory extends to non-Hamiltonian systems, so it can be relevant for small, smooth, perturbations of a family of systems with invariant tori with flows $\dot{\phi} = \omega$, constant. For example, Baesens et al. (1991) corresponds to the case here where $n = 2$ and perturbations are small.

In Section 2 we introduce a class of delay differential systems arising in neural dynamics that naturally possess high dimensional ($n = 2, 3, \dots$)

stable hyperbolic invariant tori. These occur naturally, and the relevance of the invariant tori dynamics (exhibiting sequences of spiky pulses at various nodes within a directed irreducible network) and their possible response (entrainment) to various similar forcing spiked impulses from outside (from other external nodes), is critical to their performance as (non binary) information processors. We feel that it is exciting to see this field of dynamical systems theory become critical to our understanding of novel information processing paradigms.

In Section 3 we examine the case where $n = 2$, assuming the perturbations are relatively rigid, that is, they cannot increase the winding number about a toroidal axis beyond one, as any of the phase variables goes through a single cycle. This is the case in Figure 1, where the resulting phase transition map is of the form

$$\begin{aligned}\phi'_1 &= \epsilon F_1(\phi_1, \phi_2) \\ \phi'_2 &= \phi_2 + \epsilon F_2(\phi_1, \phi_2).\end{aligned}$$

Here F_1 and F_2 are continuous doubly periodic (nonlinear) terms and ϵ is a parameter controlling their amplitude, whilst ϕ_2 represents the toroidal angle coordinate rotating around the z axis and ϕ_1 represents the toroidal angle coordinate rotating around the toroidal axis (the circle of radius 3 in the (x, y) plane about the origin). The point is that as ϕ_2 cycles so does ϕ'_2 . Yet, when either ϕ_1 or ϕ_2 cycles, ϕ'_1 does not cycle. So if we allow $\epsilon \rightarrow 0$, so that the hole at $(\phi'_1, \phi'_2) \sim (1.5, 0)$ is allowed to close up, we end up with a perturbed linear map that is not homotopic to the identity map.

2 A motivating application from delay differential equations

Consider the delay coupling of m excitable systems via an irreducible directed network. Such a model is currently being employed elsewhere (Grindrod et al., 2014) to discuss the behavioural possibilities of medium sized neuron networks within brains.

Suppose we have a very large directed graph representing neuron-to-neuron couplings. Each neuron may receive input from some smallish set of immediately upstream neurons, that are firing, while its own firing influences a smallish subset of immediately downstream neurons.

Now suppose the global network contains a maximal irreducible subgraph (a MISG). A subgraph of m neurons, represented by m vertices (v_1, \dots, v_m) and their set of interconnecting directed edges, is irreducible (often called strongly coupled) if there is a directed path between any pair of those vertices. This merely implies that every vertex can influence every other vertex via an edge-to-edge connecting path. Let A denote the corresponding adjacency matrix (where $A_{ij} = 1$ if and only if there is a directed

edge from vertex v_i to vertex v_j). The graph is irreducible if and only if $(I - \alpha A)$ is strictly positive for any $0 < \alpha < 1/\rho(A)$, so it is easy to check for irreducibility. An irreducible subgraph of some larger graph, G , is maximal if no further vertices in G can be added to the subgraph whilst retaining the property of irreducibility. When this is so then all vertices in G but not in the MISG are partitioned into (a) upstream vertices: those vertices that possess a directed path from themselves to any vertex (and thus all vertices) of the MISG; (b) downstream vertices: those vertices that possess a directed path from any vertex (and thus all vertices) of the MISG that terminate at themselves; (c) other vertices. The point being here that there can be no vertices (in G) outside of the MISG satisfying both (a) and (b).

An MISG embedded within a larger directed graph, G , can act as a processor (receiving information presented by the activity of upstream neurons, and thus upstream MISGs) responding in some dynamically coherent fashion or not, and then passing out information via its own activity onto downstream neurons, and thus downstream MISGs. We wish to clarify the type of dynamical behaviour that may be exhibited by MISGs. Typically, in isolation, these are systems with attracting invariant tori of some dimension n . In addition, we would like to understand how they might interact, typically via some type of entrainment (coherence) and nonlinear phase-locking between the MISGs own dynamic and that of its driving connections immediately upstream. This requires insights about phase entrainment possible on \mathbb{T}^n .

The models of MISGs are not very complicated, yet the behaviour can be sophisticated. Let us consider a directed MISG with m vertices $\{v_1, \dots, v_m\}$ and a corresponding adjacency matrix A . At the j th vertex we impose an excitable (and refractory) dynamical system controlling its firing behaviour. For example we might use Hodgkin-Huxley, FitzHugh-Nagumo or other ordinary differential equations. These typically contain a variable $x(t)$ corresponding to the cell membrane potential, and a number of ion concentrations, called “recovery” variables, say $\mathbf{y}(t)$. The coupling between neurons will be assumed to be dominated by the spikes in membrane potential, which are propagated as waves to and from connecting synapses, rather than via the ionic currents (which act more locally to support and then recover a passing pulse in membrane potential). The travel times for such waves result in time-delays. So there is a lag between a particular neuron firing and any of its downstream connections receiving some stimulus from it. Typically such time lags will be much larger than that of duration of individual firing pulses (the spikes in membrane potential).

We must consider systems of the form

$$\dot{x}_j(t) = f(x_j(t), \mathbf{y}_j(t)) + \mu \sum_{i=1}^m A_{ij} x_i(t - l_{ij}),$$

$$\dot{\mathbf{y}}_j(t) = \mathbf{g}(x_j(t), \mathbf{y}_j(t)),$$

for neurons $j = 1, \dots, m$. Here $\mu > 0$ is a constant coupling parameter while the $l_{ij} > 0$ denote the positive time lags between neuron i and neuron j .

Under any initial perturbation, if there is no coupling present ($\mu = 0$) then such systems will return to their resting equilibrium and stay there. With sufficient coupling present it is possible that any neurons arranged in a simple cycle within the directed graph (by definition having no repeated edges or vertices) may fire in sequence, and thus settle down into a periodic and sequential firing pattern. Of course, since the MISG is irreducible, all such simple cycles must affect one another in some way, so it is possible that not all elementary cycles will support oscillatory behaviour simultaneously. When we numerically solve such nonlinear delay differential equations, following a “kick start” initial perturbation at one or more of its vertices, we obtain long time behaviour that is asymptotic to some multiply periodic pattern equivalent to a “winding” dynamic on an attractor isomorphic to \mathbb{T}^n . By “winding” here we mean that there are n phase variables, ϕ , and the orbits on the attractor simply wind around the torus with respect to all phases: say $\dot{\phi} = \omega$, some constant positive vector. Given the long run behaviour of such a system (following a kick start) we may observe the pseudo-periodic behaviour of the m states (the x_j ’s say) and estimate the dimension n of the attractor. In such numerical examinations for more than 6000 MISGs (keeping the in-out degree distribution the same) the distribution of observed (inferred) values for n was increasing though scaled sub-linearly with the size m of the MISG (Grindrod et al., 2014). Indeed the modal values of $P(n|m)$ appears $\sim \log m$.

An examination of the effect of the quasi periodic behaviour of one MISG driving that of another MISG, immediately downstream, thus poses the question: how does the concept of phase transition maps, so well known for periodically forced limit cycles, generalize to attractors represented by winding maps over \mathbb{T}^n ? In applications such as these, a knowledge of such behaviour is essential in developing any understanding of how a reducible macro-network of MISGs might process information, with each MISG acting as an analogue filter, relay/switch, and router of certain types of stimulus.

3 Phase transition mappings for invariant \mathbb{T}^2

The two dimensional torus, $\mathbb{T}^2 = \mathbb{S}^1 \times \mathbb{S}^1$ is described by two 2π -periodic coordinates, $\phi = (\phi_1, \phi_2)^T$. We may depict \mathbb{T}^2 , in Figure 3 for example, as a two dimensional square $[-\pi, \pi]^2$ where pairs of points on opposite boundaries are identified together.

Consider the mapping, $M : \mathbb{T}^2 \rightarrow \mathbb{T}^2$, given by

$$\phi' = M(\phi) = W\phi + \epsilon\mathbf{F}(\phi) \tag{1}$$

where $\mathbf{F} = (F_1, F_2)^T$ and $W \in \{0, 1\}^{2 \times 2}$ is a matrix of winding numbers controlling the linear terms. Here F_1 and F_2 are continuous doubly periodic (nonlinear) terms and ϵ is a small positive parameter controlling their amplitude.

The restriction on W to contain only binary values is motivated by the kind of near rigid perturbation ideas contained in the examples of the Type-0/Type-1 perturbations of a limit cycle. Of course we could allow $W \in \mathbb{Z}^{2 \times 2}$ in (1) and we would generate valid maps of the torus onto itself. However, perturbations acting on the underlying state-space, containing the torus, are likely to be limited to near affine maps and relatively ‘rigid’ such that they are not exotic enough to produce additional windings. Thus, we shall consider only binary values in W ; such values could be obtained via affine perturbation maps. Nevertheless, in any particular example inducing higher winding numbers, similar considerations to those given below would apply.

For example, consider

$$\phi_1' = w_{1,1}\phi_1 + w_{1,2}\phi_2 + \epsilon F_1(\phi_1, \phi_2) \quad (2)$$

$$\phi_2' = w_{2,1}\phi_1 + w_{2,2}\phi_2 + \epsilon F_2(\phi_1, \phi_2). \quad (3)$$

In Figure 3 we take $F_1(\phi_1, \phi_2) = \sin(\phi_1 + 2\pi\alpha_1) \sin(\phi_2 + 2\pi\alpha_2)$ and $F_2(\phi_1, \phi_2) = \sin(\phi_1 + 2\pi\alpha_3) \sin(\phi_2 + 2\pi\alpha_4)$ where $\alpha = (\alpha_1, \dots, \alpha_4)$ is constant (each independently drawn, $\alpha_i \sim U[0, 1]$). We show the resulting range of M conditional on the winding numbers in W . There are 2^{n^2} possibilities for W , giving sixteen possibilities for this case, though this number can be reduced by symmetry considerations. (Here, we have ten distinct W matrices.)

Since $\mathbf{F} : \mathbb{T}^2 \rightarrow \mathbb{R}^2$ is continuous and doubly periodic $M(\phi)$ is trivially *homotopic* to the linear mapping $\phi \rightarrow W\phi$. Furthermore when the determinant of W is ± 1 the linear map is area preserving; when it is zero the range of the linear map is a simple periodic curve. This is clear in Figure 3, where we see that when $\det(W) = 0$ the nonlinearity $\epsilon\mathbf{F}$ provides a perturbation to each of the possible simple periodic curves on the torus.

Suppose that \mathbb{T}^2 is an asymptotically stable invariant attractor for some dynamical system over \mathbb{R}^m ($m \geq 3$), parametrized by 2π -periodic phase coordinates, $\phi = (\phi_1, \phi_2)^T$. Suppose further that the coordinates have been scaled so that the dynamic restricted to \mathbb{T}^2 results in a uniform rotation:

$$\dot{\phi} = \omega,$$

for a given real vector $\omega = (\omega_1, \omega_2)^T$.

Consider an instantaneous perturbation applied to \mathbb{T}^2 defined by the map M given in (1), where $\epsilon \geq 0$ is *strength* parameter controlling the nonlinear component, \mathbf{F} , which is continuous and 2π -periodic in both arguments. If this phase resetting perturbation is applied iteratively to orbits of the dynamical system, every $p > 0$ units of time, then the relationship between

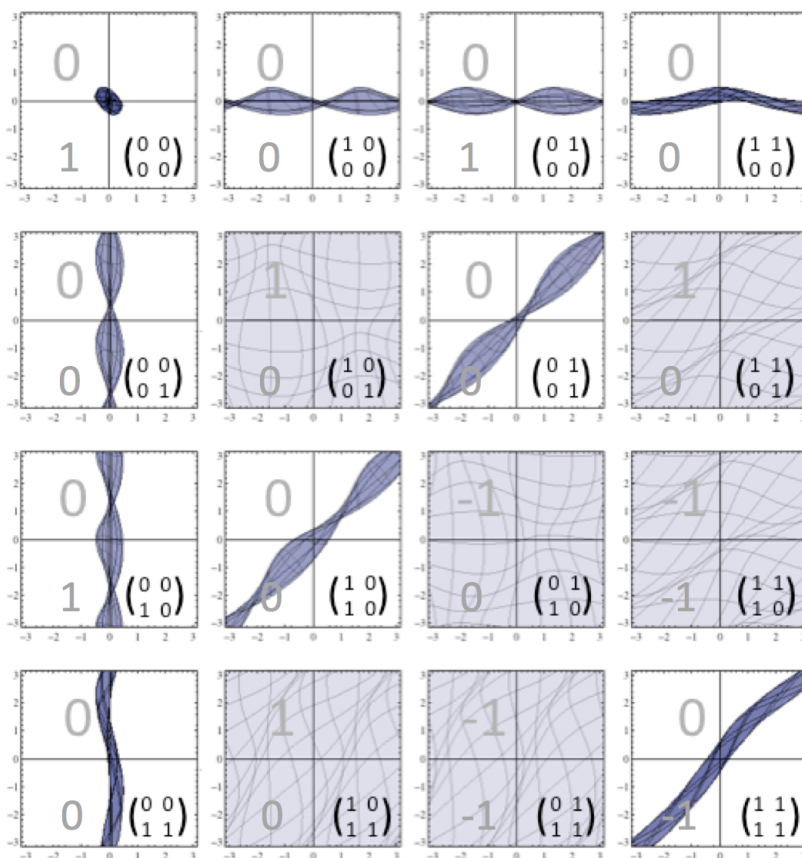


Figure 3: The range (ϕ'_1, ϕ'_2) of the mapping M as ϕ varies over \mathbb{T}^2 , for various winding number matrices, W , (bottom right); with $\det(W)$ (in grey, top left) and $\det(I - W)$ (in grey, bottom left); for parameters $\epsilon = 0.5$ and $\alpha = (0.7731\dots, 0.9082\dots, 0.9496\dots, 0.5056\dots)^T$.

the phases immediately prior to successive perturbations is given by

$$\phi^{[i+1]} = p\omega + W\phi^{[i]} + \epsilon\mathbf{F}(\phi^{[i]}) \pmod{2\pi}. \quad (4)$$

Hence there is a phase-locked, p -periodic, solution if and only if $\phi^{[i]} = \phi$ and (p, ϵ) satisfies

$$(I - W)\phi = p\omega + \epsilon\mathbf{F}(\phi) - 2\pi\mathbf{k}, \quad (5)$$

for some $\mathbf{k} = (k_1, k_2)^T \in \mathbb{Z}^2$ and $\phi \in \mathbb{T}^2$.

Let $(\phi^*, \epsilon^*, p^*, \mathbf{k}^*)$ be such a phase locked solution of (5). Then it is a linearly stable solution of (4) if and only if the spectrum of the linearised mapping $W + \epsilon^*\mathbf{dF}(\phi^*)$ lies within the unit circle. Here $\mathbf{dF}(\phi^*)$ denotes the Jacobian of $\mathbf{F}(\phi)$ evaluated at ϕ^* .

If $(I - W)$ is invertible (in 6 out of the 16 cases in Figure 3) then (5) can be solved asymptotically in the limit $\epsilon \rightarrow 0$. Let $\phi_0(p) = (I - W)^{-1}(p\omega - 2\pi\mathbf{k}) \pmod{2\pi}$. In all cases the resolvent term contains only integers so $\phi_0(p) = p(I - W)^{-1}\omega \pmod{2\pi}$ is unique. Then we have a regular expansion:

$$\begin{aligned} \phi(\epsilon, p) &= \phi_0(p) + \epsilon(I - W)^{-1}\mathbf{F}(\phi_0(p)) + \\ &\quad \epsilon^2(I - W)^{-1}\mathbf{dF}(\phi_0(p))(I - W)^{-1}\mathbf{F}(\phi_0(p)) + O(\epsilon^3). \end{aligned}$$

For all $p > 0$, as ϵ increases we thus have a unique fixed point corresponding to a phase locked solution.

This is not the case when $(I - W)$ is not invertible. $W = I$ is a standard case where a tongue of phase-locked solutions may reach $\epsilon = 0$ if and only if elements ω_1 and ω_2 are rationally related.

When $W \neq I$ yet $(I - W)$ is singular, there are tongues that can reach all the way down to the $\epsilon = 0$ for certain phase-locked values for p , regardless of ω_1 and ω_2 being rationally related. These phase-locked values may be obtained directly from the solvability condition of the limiting equation (from (5)) as $\epsilon \rightarrow 0$:

$$(I - W)\phi = p\omega - 2\pi\mathbf{k}.$$

The right-hand side must be orthogonal to the null space of $(I - W)^T$. In all such cases this yields the phase-locked values (and tongues) shown in Figure 4, along with the corresponding entrainment formulae.

4 Phase locking on \mathbb{T}^n

Suppose \mathbb{T}^n is an invariant attractor for some dynamical system over \mathbb{R}^m ($m \geq n+1$), parametrized by n 2π -periodic phase coordinates, $\phi = (\phi_1, \phi_2, \dots, \phi_n)^T$. Suppose further that the coordinates have been scaled so that the dynamic restricted to \mathbb{T}^n is a uniform rotation:

$$\dot{\phi} = \omega,$$

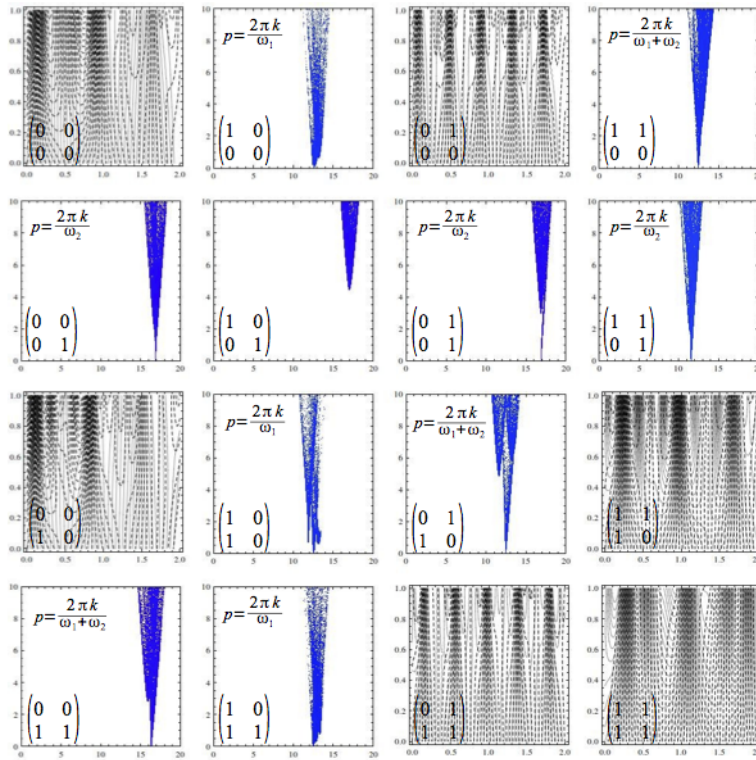


Figure 4: Phase locked solutions in the (p, ϵ) -plane. Phase-locked tongues in the cases where $(I - W)$ is singular; and entrainment at all possible (p, ϵ) -values in the cases where $(I - W)^{-1}$ exists, showing the contours of both ϕ_1 and ϕ_2 . Results are given for each W as shown bottom left.

for a given real vector $\omega = (\omega_1, \omega_2, \dots, \omega_n)^T$.

Now consider a p -periodic instantaneous perturbation that is defined by a map, $M : \mathbb{T}^n \rightarrow \mathbb{T}^n$, given by

$$M(\phi) = W\phi + \epsilon \mathbf{F}(\phi),$$

where $W \in \{0, 1\}^{n \times n}$, and $\epsilon \geq 0$ is *strength* parameter for the nonlinear term \mathbf{F} , that is itself smooth and 2π -periodic in all arguments. If this phase resetting perturbation is applied iteratively to orbits of the dynamical system, every $p > 0$ units of time, then the relationship between the phases immediately prior to successive perturbations is given by the n dimensional analog of (4):

$$\phi^{[i+1]} = p\omega + W\phi^{[i]} + \epsilon \mathbf{F}(\phi^{[i]}) \pmod{2\pi}. \quad (6)$$

Hence there is a phase-locked, p -periodic, solution if and only if (p, ϵ) satisfies

$$(I - W)\phi = p\omega - 2\pi \mathbf{k} + \epsilon \mathbf{F}(\phi), \quad (7)$$

for some $\mathbf{k} = (k_1, \dots, k_n)^T \in \mathbb{Z}^n$ and $\phi \in \mathbb{T}^n$. For $n \geq 3$ this invokes the *solvability condition*, that

$$2\pi \mathbf{k} + (I - W)\phi, \omega, \text{ and } \mathbf{F}(\phi) \text{ are coplanar,} \quad (8)$$

which defines a localised sub-section of \mathbb{T}^n where this is true. For $n = 1, 2$ there is no active solvability condition and hence $\phi \in \mathbb{T}^n$ parametrizes the possible phase locked solutions.

For $n > 2$, the solvability condition means that ϕ can not vary freely over the torus (it must live on some locally two dimensional surface). Thus the tongues plotting phase locked solutions in the (p, ϵ) plane must contain this extra ‘‘folding’’ structure within them, and thus certain multiplicities of solutions, whether reaching all the way down to $\epsilon = 0$ (at specific values of p) when $W \neq I$ yet $\det(I - W) = 0$, or when $W = I$ and elements of ω happen to be rationally related. Similarly, if $\det(I - W)$ is non-zero, phase locked solutions can exist for all p and ϵ greater than zero, though again with some more complicated structures and thus multiplicities (than in Figure 4) owing to the active solvability condition.

For $n \geq 3$, (7) and (8) imply

$$2\pi \begin{pmatrix} \omega^T(2\pi \mathbf{k} + (I - W)\phi) \\ \mathbf{k}^T(2\pi \mathbf{k} + (I - W)\phi) \end{pmatrix} = \begin{pmatrix} \omega^T \omega & \omega^T \mathbf{F}(\phi) \\ \mathbf{k}^T \omega & \mathbf{k}^T \mathbf{F}(\phi) \end{pmatrix} \begin{pmatrix} p \\ \epsilon \end{pmatrix}.$$

For example consider the case where $n = 3$, $W = I$, and $\omega = (1, 5\sqrt{2}, 2\pi)^T$. Then solvability condition (8) is non trivial, requiring that the scalar triple product, $\mathbf{F}(\phi) \cdot (\mathbf{k} \times \omega)$, vanishes.

For the choice $\mathbf{k} = (1, 7, 6)^T$, which is almost co-linear with ω , we expect that there may be solutions for (7) close to $p = 2\pi$ with ϵ very small.

Yet observe Figure 5, which shows the numerical phase-locked solutions in the (p, ϵ) -plane; the solutions appear very different from the simple tongues observed above for $n = 1$ and 2. The solvability condition restricts ϕ to a (locally) two dimensional subset of \mathbb{T}^3 . For such ϕ values we depict the corresponding phase-locked solutions in the first quadrant of the (p, ϵ) -plane, along with their stability.

Consider the following example, where $\mathbf{F}(\phi)$ has been generated with random phase- shifts and amplitudes chosen from uniform distributions, over $[0, 2\pi)$ and $[0, 1)$ respectively, and is given in the appendix. Then, in Figure 6 we show the subset of \mathbb{T}^3 satisfying the solvability condition and the equivalent tongue of phase-locked solutions in the (p, ϵ) -plane is exactly that of Figure 5.

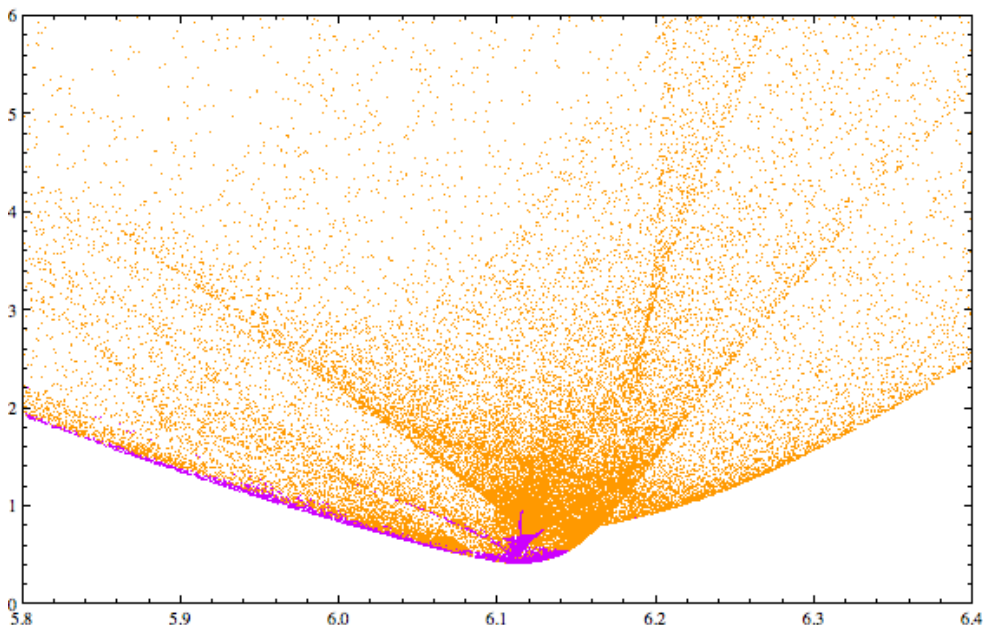


Figure 5: Stable (dark) and unstable (light) phase-locked solutions: ϵ vs p .

5 Conclusion

The fast-slow partition of dynamics is a very standard way to consider dynamical systems exhibiting large excursions and/or subject to large perturbations from an attractor. In this case we have generalised the phase transition mapping concept, and the consequent entrainment behaviour, that was known for clocks (attractors homeomorphic to a circle, \mathbb{T}^1) to systems with attractors homeomorphic to \mathbb{T}^n . For large, near rigid, perturbations (those not increasing the winding numbers), it is reasonable that the phase transition mappings are homotopic to one of 2^{n^2} linear maps, represented

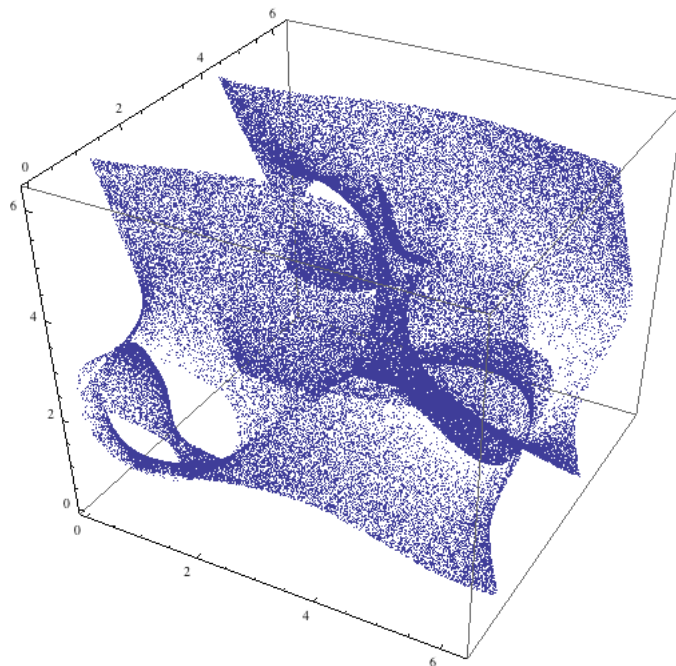


Figure 6: Locus of $\phi \in \mathbb{T}^3$ satisfying the solvability condition $\mathbf{F}(\phi) \cdot (\mathbf{k} \times \boldsymbol{\omega}) = 0$.

by binary $n \times n$ matrices W . The dimension of the null space of $(I - W)$ determines the possible entrainment behaviour of the system when the phase transition mapping (largish for perturbations) is applied successively with period p , as the nonlinear component of the transition mapping, scaled by $\epsilon > 0$, increases from zero.

For $n = 2$ the situation is relatively straightforward in our chosen notation. We can think of searching for those pairs (p, ϵ) for which entrainment is possible where the perturbations are applied at atleast one value of ϕ . For $n \geq 3$ things are further complicated by an additional solvability condition that restricts the possibility for the entrainment to phases on some two dimensional sections through \mathbb{T}^n .

In future work we wish to apply these ideas within the analysis of systems such as the delay differential equations modelling MISGs discussed within Section 2. A huge collection of sparsely coupled MISGs is a starting point to consider the non-binary processing of information, locally by each MISG subject to inputs from, and with outputs to, other MISGs. Since such DDEs on directed irreducible subgraphs contain (many) cycles that together give rise naturally to toroidal attractors, the investigation of their phase response to periodic upstream stimuli, and the possible entrainment of their behaviour, is essential.

References

- C. Baesens, J. Guckenheimer, S. Kim, and R. S. MacKay. Three coupled oscillators: mode-locking, global bifurcations and toroidal chaos. *Physica D: Nonlinear Phenomena*, 49(3):387–475, 1991.
- E. Brown, J. Moehlis, and P. Holmes. On the phase reduction and response dynamics of neural oscillator populations. *Neural Computation*, 16(4):673–715, 2004.
- G. B. Ermentrout. Type I membranes, phase resetting curves, and synchrony. *Neural Computation*, 8(5):979–1001, 1996.
- G. B. Ermentrout and N. Kopell. Oscillator death in systems of coupled neural oscillators. *SIAM Journal on Applied Mathematics*, 50(1):125–146, 1990.
- L. Glass and M. C. Mackey. *From Clocks to Chaos: The Rhythms of Life*. Princeton University Press, 1988.
- P. Goel and G. B. Ermentrout. Synchrony, stability, and firing patterns in pulse-coupled oscillators. *Physica D: Nonlinear Phenomena*, 163(3):191–216, 2002.
- P. Grindrod, Z. V. Stoyanov, G. M. Smith, and J. D. Saddy. Resonant behaviour of irreducible networks of neurons with delayed coupling. *Physica D*, 2014. Submitted.
- M. R. Guevara, A. Shrier, and L. Glass. Phase resetting of spontaneously beating embryonic ventricular heart cell aggregates. *Am. J. Physiol*, 251(6):H1298–H1305, 1986.
- R. S. MacKay. Transition of the phase-resetting map for kicked oscillators. *Physica D: Nonlinear Phenomena*, 52(2):254–266, 1991.
- J. Rinzel and G. B. Ermentrout. Analysis of neural excitability and oscillations. In C Koch and I Segev, editors, *Methods in Neuronal Modeling: From Synapses to Networks*, pages 135–169. Cambridge MA, MIT Press, 1989.
- A. T. Winfree. *The geometry of biological time*, volume 12. Springer, 2001.

Appendix

Here is the nonlinear part of the phase transition mapping for \mathbb{T}^3 employed in the example given in Figures 6 and 5 (shown to two decimal places). We

have $\mathbf{F}(\phi) = (F_1, F_2, F_3)^T$ given by

$$\begin{aligned} F_1 &= 0.63 \sin(\phi_1 + 1.41) \sin(\phi_2 + 3.53) \sin(\phi_3 + 0.72) + \\ &\quad 0.09 \sin(\phi_1 + 0.65) \sin(\phi_2 + 5.52) + \\ &\quad 0.84 \sin(\phi_1 + 3.15) \sin(\phi_3 + 5.51) + 0.35 \sin(\phi_1 + 3.15) + \\ &\quad 0.72 \sin(\phi_2 + 1.73) \sin(\phi_3 + 2.18) + 0.95 \sin(\phi_2 + 1.68) + 0.28 \sin(\phi_3 + 5.86), \\ F_2 &= 0.44 \sin(\phi_1 + 3.76) \sin(\phi_2 + 5.89) \sin(\phi_3 + 5.94) + \\ &\quad 0.07 \sin(\phi_1 + 0.25) \sin(\phi_2 + 3.65) + \\ &\quad 0.53 \sin(\phi_1 + 0.83) \sin(\phi_3 + 5.93) + 0.44 \sin(\phi_1 + 1.02) + \\ &\quad 0.47 \sin(\phi_2 + 1.83) \sin(\phi_3 + 4.11) + 0.57 \sin(\phi_2 + 6.22) + 0.85 \sin(\phi_3 + 5.11), \\ F_3 &= 0.62 \sin(\phi_1 + 0.49) \sin(\phi_2 + 3.87) \sin(\phi_3 + 3.45) + \\ &\quad 0.55 \sin(\phi_1 + 5.13) \sin(\phi_2 + 0.39) + \\ &\quad 0.67 \sin(\phi_1 + 4.63) \sin(\phi_3 + 4.72) + 0.17 \sin(\phi_1 + 6.07) + \\ &\quad 0.03 \sin(\phi_2 + 1.27) \sin(\phi_3 + 0.59) + 0.71 \sin(\phi_2 + 2.39) + 0.051 \sin(\phi_3 + 3.28). \end{aligned}$$